

Two-dimensional and three-dimensional simulation of wave interaction with an Oscillating Wave Surge Converter

Ashkan Rafiee & Frederic Dias*
School of Mathematical Sciences
University College Dublin, Belfield Dublin 4, Ireland.
email: ashkan.rafiiee@ucd.ie & frederic.dias@ucd.ie

Introduction and aim of the work

As the energy demand and the shortage in the world oil supplies are significantly increasing, new challenges arise in the current geopolitical situation. On the other hand, the global warming and economical situation of the world have significantly increased the need for a green energy generated from the renewable sources. Renewable sources such as wind and solar energies have been developed for the past few decades and there has been significant progress in harnessing energy from these sources. However, due to the importance of location on the power densities associated with these sources the demand for alternative renewable energy sources has increased.

During the 1970's global oil crisis, ocean waves were considered as a potential source of energy [1]. Nevertheless, due to the complicated nature of water wave interaction with floating/tethered bodies, the wave energy technology has not yet achieved a universal standard conceptual design similar to wind energy turbines. Therefore, various wave energy devices have been developed and deployed to harness the energy of water waves.

One of the most promising wave energy converter devices is the bottom hinged Oscillating Wave Surge Converter (OWSC). It has been known that bottom hinged OWSCs are an efficient way of extracting power from ocean waves [2]. OWSCs are in general large buoyant flaps, hinged at the bottom of ocean and oscillating back and forth under the action of incoming incident waves [3, 4]. The oscillating motion is converted into energy by pumping high pressure water to drive a hydro-electric turbine [5]. OWSCs are shallow water devices and hence the interacting waves have large horizontal velocity component. This results in a strong wave load on these devices. Therefore, large amplitude oscillations are expected. In some cases slamming can occur but this is the sub-

ject of work in progress. Hereby, the widely used potential flow theories are not sufficient to simulate wave interaction with OWSCs.

In this paper, the wave load on an OWSC will be studied using the Smoothed Particle Hydrodynamics (SPH) method. SPH method is a meshless, purely Lagrangian technique which was originally developed in 1977 by Lucy [6] and Monaghan and Gingold [7]. It has subsequently been successfully employed in a wide range of problems, e.g. astrophysics, fluid mechanics, solid mechanics, fluid-structure interaction and many more (see [8] for a recent review).

Mathematical model

The governing equations of transient compressible fluid flow include the conservation of mass and momentum equations. In this work, the governing equations are written in a Lagrangian framework as

$$\frac{1}{\rho} \frac{d\rho}{dt} + \nabla \cdot \mathbf{v} = 0 \quad (1)$$

$$\frac{d\mathbf{v}}{dt} = -\frac{1}{\rho} \nabla p + \nabla \cdot (\nu \nabla \mathbf{v}) + \mathbf{g}$$

where ρ , t , \mathbf{v} , p , ν and \mathbf{g} are density, time, velocity vector, pressure, kinematic viscosity and gravitational acceleration, respectively. The coordinates are X along the channel, Y along the vertical and Z across the channel.

In order to take into account the effects of turbulence on the flow, turbulent fluctuations are modelled through the concept of eddy viscosity estimated from the well-known and widely used $k - \epsilon$ model. The Lagrangian form of the Reynolds average Navier-Stokes (RANS) equations with $k - \epsilon$ turbulence model

*Presenting author

read [9]

$$\frac{d\rho}{dt} = -\rho \nabla \cdot \mathbf{v}$$

$$\frac{d\mathbf{v}}{dt} = -\frac{1}{\rho} \nabla \tilde{p} + \nabla \cdot \left[\left(\nu + \nu_T \right) \nabla \mathbf{v} \right] + \mathbf{g}$$

$$\frac{dk}{dt} = P - \epsilon + \nabla \cdot \left[\left(\nu + \frac{\nu_T}{\sigma_k} \right) \nabla k \right] \quad (2)$$

$$\frac{d\epsilon}{dt} = \frac{\epsilon}{k} \left(C_{\epsilon,1} P - C_{\epsilon,2} \epsilon \right) + \nabla \cdot \left[\left(\nu + \frac{\nu_T}{\sigma_\epsilon} \right) \nabla \epsilon \right]$$

$$\frac{d\mathbf{r}}{dt} = \mathbf{v}$$

where $\tilde{p} = p + 2/3\rho k$ is the modified pressure and $\nu_T = C_\mu k^2/\epsilon$ is the eddy viscosity. The production of turbulent energy P is given by

$$P = \nu_T \mathbf{S} : \mathbf{S} \quad (3)$$

where the rate-of-strain tensor \mathbf{S} takes the form

$$\mathbf{S} = \frac{1}{2} \left[\nabla \mathbf{v} + (\nabla \mathbf{v})^T \right]. \quad (4)$$

The standard $k - \epsilon$ model constants are

$$\begin{aligned} C_\mu = 0.09; \quad C_{\epsilon,1} = 1.44; \quad C_{\epsilon,2} = 1.92; \\ \sigma_k = 1.0; \quad \sigma_\epsilon = 1.3. \end{aligned} \quad (5)$$

Results

The SPH simulations of OWSC were carried out in a 20 m long wave tank. The regular wave is modelled using a piston-type wave maker located at the left end of the tank. The displacement of the piston-type wavemaker is determined by the linear wavemaker theory [10]

$$X(t) = A_0 \sin(\omega t) \quad (6)$$

where

$$A_0 = \frac{an_1}{\tanh(kh_0)}; \quad n_1 = \frac{1}{2} \left(1 + \frac{2kh_0}{\sinh(2kh_0)} \right). \quad (7)$$

Here, a , k , ω and h_0 are the wave amplitude, wave number, wave frequency and the initial water depth, respectively.

A dissipation zone is used for damping the wave amplitude at the right end of the tank. In this dissipation region, a friction source term is added to the vertical velocity component within the momentum equation. In order to avoid the velocity damping

in the uniform horizontal flow, the damping force in the horizontal direction was not considered.

The dimensions of the OWSC model and the wave tank were similar to the ones described in [3] and a 2D schematic is shown in Fig. 1. The SPH particles were initially placed on a grid of squares with initial spacing of $l_0 = 0.022$ m and $l_0 = 0.033$ m for 2D and 3D simulations, respectively. In both cases the SPH smoothing length was set to $h = 1.5l_0$ and the boundary particles were placed with the spacing of $l_0/3$.

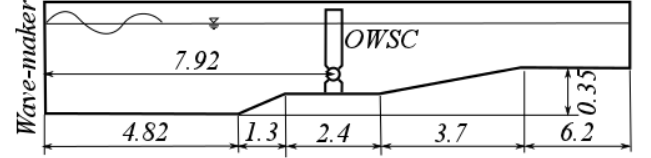


FIGURE 1: A two-dimensional schematic of the wave tank and the OWSC model. the dimensions are in meter.

The wavemaker was calibrated to produce regular waves with a 0.12 m wave height and a 2 s period. Figures 2 and 3 show snapshots of 2D and 3D SPH simulations at various times, respectively.

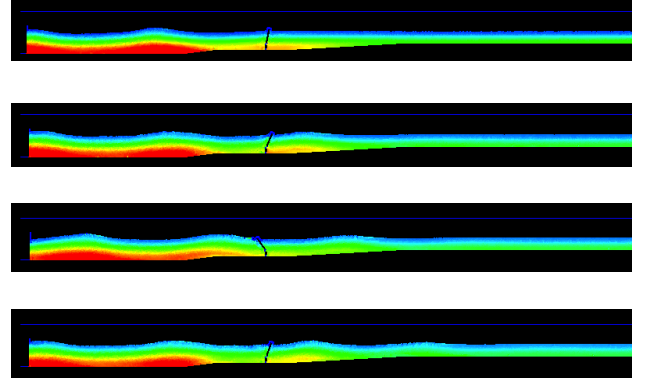


FIGURE 2: 2D SPH simulation of wave impact on an OWSC. Particles are coloured by their pressure.

By comparing Figs. 2 and 3 it can clearly be seen that after the incoming wave interacts with the OWSC, the flow is no longer 2D around the flap. Hence a 2D simulation is not sufficient to accurately predict the rotation of the flap. In order to scrutinise this further, the time variation of the flap angle is compared with experimental data obtained in the wave tank of Queen's University Belfast in Fig. 4.

As illustrated in Fig. 4, the maximum angle of rotation of the flap is under-estimated by 2D simulations whereas 3D simulations were able to capture

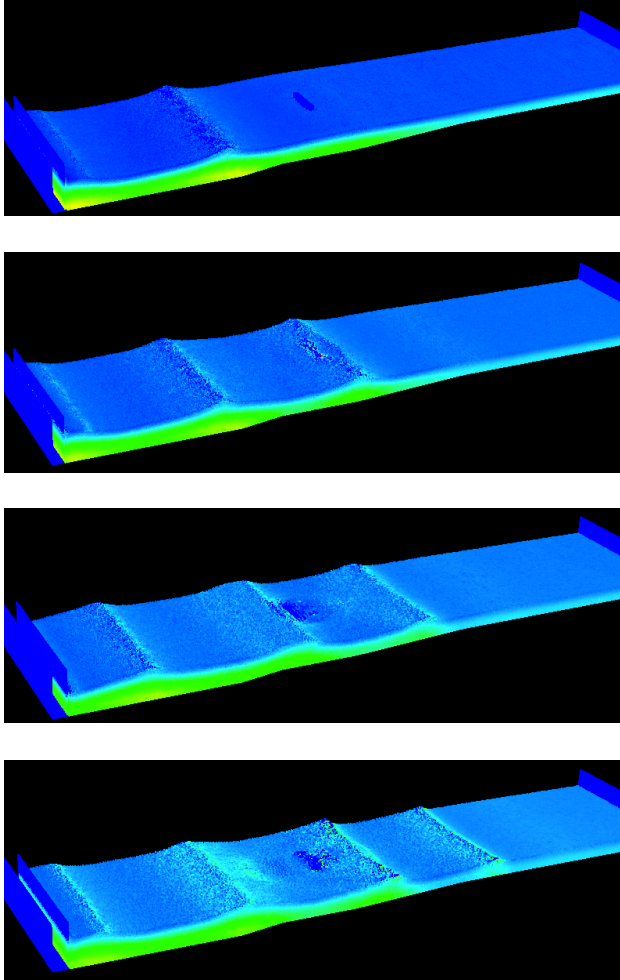


FIGURE 3: 3D SPH simulation of the interaction between incoming waves and an OWSC. Particles are coloured with their pressure.

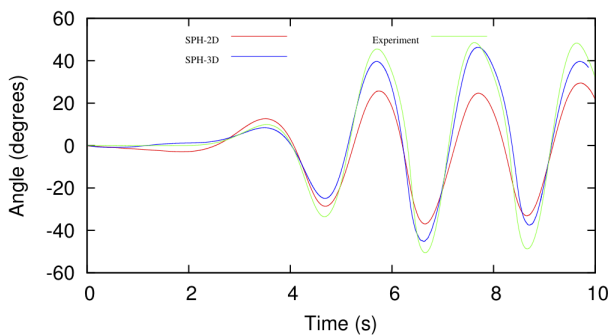


FIGURE 4: Comparison between angle of the flap from 2D and 3D simulations with experimental data.

the angle of flap more accurately.

In order to investigate the performance of OSWCs,

it is crucial to understand and to accurately predict the wave loading on them. To do so, 13 pressure transducers were mounted on the front face (toward the wavemaker) of the device during the experiments. The initial locations of the transducers are given in Tab. 1. The position along the transverse Z axis is measured from the centre of the device.

TABLE 1: Initial position of the pressure transducers on the front side of the OWSC.

| Pressure Transducer | pos Y [mm] | pos Z [mm] |
|---------------------|------------|------------|
| PT1 | 0.6655 | 0.4680 |
| PT2 | 0.4820 | 0.4680 |
| PT3 | 0.7615 | 0.3640 |
| PT4 | 0.6195 | 0.3640 |
| PT5 | 0.4360 | 0.3640 |
| PT6 | 0.6808 | 0.2600 |
| PT7 | 0.5280 | 0.2600 |
| PT8 | 0.7615 | 0.1560 |
| PT9 | 0.6195 | 0.1560 |
| PT10 | 0.4360 | 0.1560 |
| PT11 | 0.7365 | 0.0520 |
| PT12 | 0.6502 | 0.0520 |
| PT13 | 0.4973 | 0.0520 |

Figures 5 and 6 show the time history of the pressure obtained with the 2D SPH simulations at the pressure transducer locations on the OWSC. Except at the pressure transducer 2 where both 2D and 3D simulations match, 3D results show very agreement with experimental data in all the other cases. The slight discrepancies between numerical estimations of the maximum pressure peaks and the experimental data are due to their stochastic nature and to the lack of exact repeatability of the experiments.

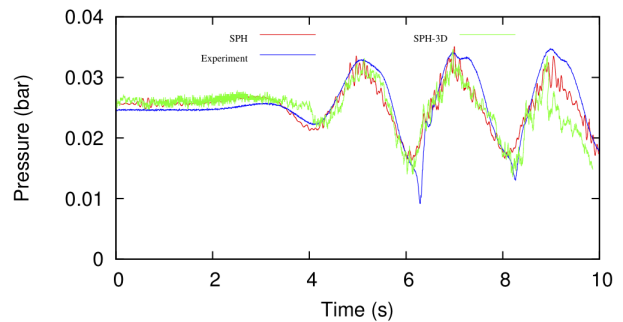


FIGURE 5: Time history of pressure variation at sensor $PT2$ in table 1.

Final Remarks

In this paper, a modified SPH method utilising a particle pair-wise Riemann solver in calculating density

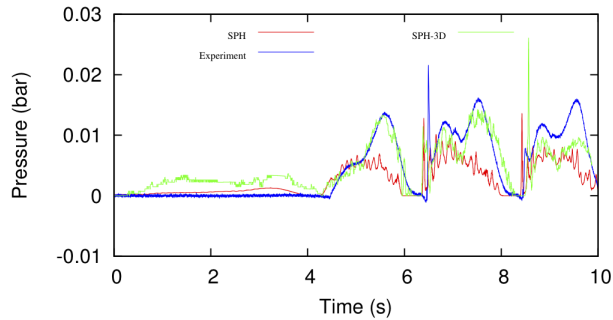


FIGURE 6: Time history of pressure variation on sensor PT11 in table 1.

filed was used to study the wave impact on an Oscillating Wave Surge Converter. In addition to capture the turbulent characteristics of the problem the Lagrangian form of the RANS $k - \epsilon$ model was included in the SPH equations. It was observed that the 3D SPH simulations resulted in a more accurate estimation of the pressure peaks on the OWSC. In addition, the time variation of the angle of rotation of the OWSC was in closer agreement with the experimental data for 3D simulations compared to the 2D simulations. The same comment applies for the total torque exerted on the flap around the hinged position (not shown here - see [11]). The main conclusion is that 3D simulations are essential to accurately estimate the loads on the OWSCs. 3D simulations with finer resolutions are currently being performed to study the effect of SPH particles size on the angle of rotation of the flap and the pressure exerted on the pressure sensors.

This work has been funded by Science Foundation Ireland (SFI) under the research project “High-end computational modelling for wave energy systems”. The authors would like to thank Irish Centre for High-End Computing (ICHEC) for the provision of computational facilities and support. Also, this work was granted access to the HPC resources of Swiss National Supercomputing Centre (CSCS)/Mount Rosa – Cray XE6 cluster made available within the Distributed European Computing Initiative by the PRACE-2IP, receiving funding from the European Community’s Seventh Framework Programme (FP7/2007-2013) under grant agreement n° RI-283493.

The experiments were performed at Queen’s University of Belfast and the authors would like to extend their gratitude to Dr. Sylvain Bourdier and Prof. Trevor Whittaker for kindly sharing their experimental data.

References

- [1] M. Folley, T. Whittaker, and M. Osterried, “The Oscillating Wave Surge Converter,” in *The 14th International Offshore and polar Engineering Conference (ISOPE)*, 2004.
- [2] T. Whittaker, D. Collier, M. Folley, M. Osterried, A. Henry, and M. Crowley, “The development of Oyster – a shallow water surging wave energy converter,” in *7th European Wave and Tidal Energy Conference*, Porto, Portugal, 2007.
- [3] P. Schmitt, S. Bourdier, D. Sarkar, E. Renzi, F. Dias, K. Doherty, T. Whittaker, and J. Hoff, “Hydrodynamic loading on a bottom hinged oscillating wave surge converter,” in *The 22nd International Offshore and Polar Engineering Conference*, Rhodes, Greece, 2012.
- [4] E. Renzi and F. Dias, “Resonant behavior of the oscillating wave surge converter in a channel,” *Journal Fluid Mechanics*, vol. 701, pp. 482–510, 2012.
- [5] L. Cameron, R. Doherty, A. Henry, K. Doherty, J. Hoff, D. Naylor, S. Bourdier, and T. Whittaker, “Design of the next generation of the Oyster wave energy converter,” in *3rd International Conference on Ocean Energy*, 2010.
- [6] L. B. Lucy, “A numerical approach to the testing of the fission hypothesis,” *Astron. J.*, vol. 82, pp. 1013–1020, 1977.
- [7] R. A. Gingold and J. J. Monaghan, “Smoothed particle hydrodynamics: Theory and application to nonspherical stars,” *Mon. Not. Roy. Astr. Soc.*, vol. 181, pp. 375–389, 1977.
- [8] J. J. Monaghan, “Smoothed Particle Hydrodynamics and its diverse applications,” *Annu. Rev. Fluid. Mech.*, vol. 44, pp. 323–346, 2012.
- [9] D. Violeau and R. Issa, “Numerical modelling of complex turbulent free-surface flows with the SPH method: an overview,” *Int. J. Numer. Meth. Fluids*, vol. 53, pp. 277–304, 2007.
- [10] R. G. Dean and R. A. Dalrymple, *Water wave mechanics for engineers and scientists*. Prentice-Hall, Englewood Cliffs, N.J., 1984.
- [11] A. Rafiee and F. Dias, “Numerical simulation of wave interaction with an oscillating wave surge converter,” in *Proceedings of OMAE 2013, ASME 32nd International Conference on Offshore Mechanics and Arctic Engineering*, Nantes, France, 2013.